

Article

Quantile Dependence between Crude Oil Returns and Implied Volatility: Evidence from Parametric and Nonparametric Tests

Bechir Raggad ^{1,2,3,*}  and Elie Bouri ⁴ 

¹ Department of Business Administration, College of Business Administration in Majmaah, Majmaah University, Majmaah 11952, Saudi Arabia

² Faculty of Economics and Management in Nabeul, University of Carthage, Carthage 2085, Tunisia

³ BESTMOD Laboratory, Higher Institute of Management of Tunis, University of Tunis, Tunis 1002, Tunisia

⁴ School of Business, Lebanese American University, Beirut P.O. Box 13-5053, Lebanon

* Correspondence: b.raggad@mu.edu.sa

Abstract: We examine the daily dependence and directional predictability between the returns of crude oil and the Crude Oil Volatility Index (OVX). Unlike previous studies, we apply a battery of quantile-based techniques, namely the quantile unit root test, the causality-in-quantiles test, and the cross-quantilogram approach. Our main results show evidence of significant bi-directional predictability that is quantile-dependent and asymmetric. A significant positive Granger causality runs from oil (OVX) returns to OVX (oil) returns when both series are in similar lower (upper) quantiles, as well as in opposite quantiles. The Granger causality from OVX returns to oil returns is only significant during periods of high volatility, although it is not always positive. The findings imply that the forward-looking estimate of oil volatility, reflecting the sentiment of oil market participants, should be considered when studying price variations in the oil market, and that crude oil returns can be used to predict oil implied volatility during bearish market conditions. Therefore, the findings have implications regarding predictability under various conditions for oil market participants.

Keywords: quantile dependence; directional predictability; granger causality in quantiles; crude oil returns; oil implied volatility

MSC: 62



Citation: Raggad, B.; Bouri, E. Quantile Dependence between Crude Oil Returns and Implied Volatility: Evidence from Parametric and Nonparametric Tests. *Mathematics* **2023**, *11*, 528. <https://doi.org/10.3390/math11030528>

Academic Editor: Francisco Jareño

Received: 8 December 2022

Revised: 7 January 2023

Accepted: 16 January 2023

Published: 18 January 2023



Copyright: © 2023 by the authors. Licensee MDPI, Basel, Switzerland. This article is an open access article distributed under the terms and conditions of the Creative Commons Attribution (CC BY) license (<https://creativecommons.org/licenses/by/4.0/>).

1. Introduction

Large price fluctuations in the crude oil market have become a staple of the last two decades, subsequent to changes in supply–demand fundamentals [1], global economic activity [2], geopolitical risk [3], and various crisis periods such as the COVID-19 outbreak [4,5]. On 20 April 2020, crude oil prices experienced huge and unprecedented turbulence, during which the price of US benchmark crude oil West Texas Intermediate (WTI) futures plunged to below USD 0 a barrel for the first time in history. This was particularly due to two main factors. The first is the slowdown in the world economy following the rapid spread of the COVID-19 pandemic, which eventually spawned a sharp decrease in crude oil demand and an oversupply of crude oil. The second is the conflict between OPEC and non-OPEC producers on the oil production level, including the oil price war between Saudi Arabia and Russia.

Oil price volatility is a major concern for consumers, corporations, and governments. This is not surprising given that oil price fluctuations potentially have considerable effects on the investment decisions of investors and corporations as well as the global economy [6–9]. Usually, volatility is computed based on historical price data using realized volatility estimators, GARCH-based models, and stochastic volatility models. Another way to compute volatility is via the so-called implied volatility, based on data from the options market. Several studies indicate that implied volatility is superior to the former models [10–13]. In this regard, one of

the indicators that investors and analysts regularly follow to assess the future state of crude oil volatility is the Chicago Board Options Exchange (CBOE) Crude Oil Volatility Index (OVX), which was introduced in 2007. OVX represents the 30-day forward-looking market estimate of volatility and is viewed as a barometer of investor sentiment about the crude oil market. Compared to historical volatility, it offers a more timely assessment of risk as it comprises both past market information and future anticipation [13,14]. Accordingly, OVX can reasonably transmit trading signals for market operators because it allows market participants to identify and link the movement of OVX to overall market confidence and panic in the crude oil market.

Interestingly, the risk-return trade-off is a crucial component of investment decisions and portfolio management. Despite the importance of this relationship, there is no clear agreement on its direction among researchers and analysts. Previous studies mainly concentrate on the relationship between returns and historical volatility in financial markets [15–19], while providing mixed results. Some show that the relationship is positive [20–22], while others find evidence of a negative relationship [23–25]. With the emergence of implied volatility and its role as a barometer of risk assessment [13,14], much attention has been paid to the return–implied volatility link in financial markets [26]. However, such research in the context of the oil market is relatively scarce. As noted by Ji and Fan [27], recommendations deduced in the stock market cannot be easily adopted to OVX in virtue of the more complex structure of crude oil options. Existing studies using OVX consider its predictive power for oil return volatility (e.g., [10,28–33]), or the spillover effect between oil and equity markets based on implied volatility indexes (e.g., [34–37]), whereas limited studies concentrate on the relationships between crude oil returns and OVX. In this regard, most studies examine the linear relationship between oil returns and OVX (e.g., [38–40]), whereas fewer consider the non-linear dependence. Agbeyegbe [41], Ji and Fan [27], Liu et al. [21], and Echaust and Just [42] use approaches based on copula models; Li et al. [43] apply a multiscale multivariate multifractal detrended fluctuation analysis; and Shaikh [44], Silva Junior [45], and Fousekis [46] use approaches based on quantile regression methods. Nevertheless, none of these studies assess the Granger causal relationship between crude oil returns and OVX based on quantile-based techniques accounting for various market conditions. Moreover, the disagreement in outcomes regarding the relationship between the two metrics indicates that the issue is still largely open to empirical investigation. In this paper, we examine the dependence and directional predictability between the returns of crude oil and OVX using daily data and various quantile-based techniques. Taking daily data from 10 May 2007 to 17 April 2020, we apply a battery of quantile-based techniques, specifically the quantile unit root test developed by Galvao [47], the causality-in-quantiles test of Troster [48], and the cross-quantilogram of Han et al. [49].

This paper contributes to the existing literature in the following ways. Firstly, to the best of our knowledge, this is the first study to cast new light on the Granger causal interaction between crude oil returns and changes in implied volatility using the quantile unit root test developed by Galvao [47], the causality-in-quantiles test of Troster [48], and the cross-quantilogram of Han et al. [49]. These tests can show whether variables are nonstationary or exhibit a heterogeneous causal structure across quantiles. Particularly, the test of Troster [48] has the merit of taking into account potential nonlinear causal links in conditional quantiles of the distribution, while the approach of Han et al. [49] is advantageous in at least two aspects. Notably, it is less prone to misspecification and takes into account large lags in the causality test. These approaches, based on a non-linear econometric framework, fit perfectly in our context, given that the causality links between oil prices and OVX are potentially non-linear and specific to market conditions and volatility states. Secondly, our analysis allows us to investigate not merely the magnitude but also the sign, duration, potential asymmetry, and Granger causal quantile of the dependence between the variables under consideration. Thirdly, the existence of causality in tails advocates the utility and significance of our modelling approach, and therefore casts doubt on the suitability of the conventional conditional mean-founded causality test, which gives only a partial picture by relying on the conditional mean.

The main findings reveal the existence of significant bi-directional predictability between oil returns and OVX. Notably, the relationship is found to be quantile-dependent and asymmetric across various market conditions. In fact, a significant positive dependence running from WTI (OVX) returns to OVX (WTI) is seen when both oil returns and oil implied volatility are in similar lower (upper) quantiles. Evidence of dependence is also reported when they are in opposite quantiles; for example, WTI returns Granger-cause OVX during extreme and moderate market conditions. For the reverse case, the relationship appears to be significant only during periods of high levels of OVX, but is not always positive. Furthermore, the quantile dependence from WTI returns to OVX is different from that from OVX to WTI returns, suggesting an asymmetry. Henceforth, investor sentiment in the oil market, as reflected by OVX, can be considered a driver of forthcoming variations in the returns in the oil market, and WTI returns affect OVX.

The rest of the paper is structured as follows. Section 2 provides a brief review of the related literature. Section 3 presents the econometric methodology. Section 4 defines the data and offers a preliminary investigation. Section 5 presents and discusses the empirical results. Section 6 concludes.

2. Literature Review

How the expected return of an investment is linked to the expected risk is widely documented in the academic literature [50]. Risk-return trade-off is an essential component of investment decisions and assessing portfolios. Interestingly, with the emergence of implied volatility [13,14], much attention has been paid to the return–implied volatility link in financial markets [26], but less evidence exists on the implied volatility in the context of the oil market.

The existing literature on OVX can be divided into three main strands. The first strand focuses on the predictive power of OVX for oil return volatility. For example, Szakmary et al. [10] find that the implied volatility (IV) is superior to the historical volatility (HV) as a predictor of the afterward realized volatility. They note that the IV embeds a significant amount of information that should be taken into consideration. Consequently, the authors propose a combined version of GARCH and IV models to improve oil volatility predictions. Likewise, Dutta [30] proves that OVX has a better predictive power for oil volatility than realized volatility (RV) measures. By incorporating GARCH models in the analysis, Agnolucci [51] shows that these models, mainly with Generalized Error Distribution (GED) residuals, outperform implied volatility (IV). In the same context, Lux et al. [29] evaluate the forecasting performance of various competing volatility models (GARCH with linear and non-linear dynamics, implied volatility, and multifractal models (MSM)), and show the superiority of MSM models over the other ones, across various forecasting horizons and sub-periods. This superiority is equally maintained in predicting the value-at-risk (VaR). Chen et al. [32] reveal that integrating OVX-based implied volatility into GARCH-type models generally ameliorates the predictive performance of volatility in crude oil market. Using the heterogeneous autoregressive-realized volatility (HAR-RV) models, Haugom et al. [28] show that econometric models can be enhanced by integrating implied volatility. Utilizing similar models, Lv [31] show evidence of the significant and positive effect of OVX on future realized volatility. Furthermore, the impact of a large OVX on future volatility is larger than a small OVX. Recently, Benedetto et al. [33] apply an entropy-based method and find a surge in the information flow between OVX and the spot variance of Brent returns and a corresponding drop in the information flow with WTI. Nevertheless, the causal flow running from the oil spot variance to OVX is larger in magnitude and more statistically significant for WTI than for Brent.

Previous studies also examine the impact of crude oil shocks on the job market [52,53], GDP [54], and the oil-food nexus [55]. On a different front, Ma et al. [56] forecast the realized volatility of oil futures. Notably, another strand of empirical studies focuses on the spillover effect between crude oil and equity markets based on implied volatility indexes. For example, Maghyreh et al. [34] investigate the directional connectedness between

oil and equities based on implied volatility indexes. The authors prove the existence of two-way information flows between the two markets, although it is stronger from the oil market to equity markets than the other way around. Bouri et al. [35] use the ARDL cointegration technique and the causality approach and suggest the existence of strong nonlinear relationships between the implied volatilities of gold and oil and that of the Indian stock market. However, their outcomes indicate no evidence of feedback link from the Indian stock market to the gold and crude oil markets. Similarly, Choi and Hong [36] use autoregressive distributed lag (ARDL) bounds and Toda–Yamamoto Granger causality tests to show that OVX and VIX exhibit a two-way causality in the period that covers the shale gas revolution, but no causal link in the period that does not. They confirm that OVX Granger-causes VKOSPI in the pre-shale gas revolution phase but fail to ascertain any causal flow between the two variables in the post-revolution phase. Recently, Naeem et al. [37] investigate the dynamic connectedness between a set of implied volatility indexes (oil (OVX), gold (GVZ), currency (EVZ), and bond (TYNVI)), and conclude that OVX is the leading driver of the inherent VIX connectedness of the global equity markets during anxiety phases.

The third strand of literature concentrates on the relationships between crude oil and OVX returns. For example, Aboura and Chevallier [38] assess the role exercised by implied volatility on the WTI crude oil price and establish that the so-called “inverse leverage effect”, which means that volatility is rising more following positive returns than following negative returns, is the main effect driving WTI crude oil price evolutions. Specifically, they argue that this stylized evidence could reflect the anxiety of oil consumers facing rising crude oil prices. Chen et al. [39] employ a Kalman filter with time varying coefficients in the regression equations and find a feeble negative link between OVX changes and future crude oil price returns, and that extreme values (high or low) of OVX cannot correctly forecast future evolutions of returns (positive or negative). Using copula quantile regressions, Agbeyegbe [41] show an inverted U-shaped relationship between oil returns and OVX, suggesting a stronger connection at the tails of the distribution than at the central part. Similarly, Ji and Fan [27] investigate the causal links between WTI returns and OVX and find evidence of a strong unidirectional causal link in-mean (in-variance) from WTI returns (OVX changes) to OVX changes (WTI returns). They also show that the contemporaneous relation between them is negative and asymmetric, which discloses that OVX manifests as a gauge of investor fear than as risk preference. Liu et al. [21] use copula models and find that WTI returns and OVX are mostly negatively linked. They note the presence of significant risk flows from OVX to WTI. In an analogous manner, Silva Junior [45] studies the relationship between United States Oil Fund (USO) returns and OVX, employing ordinary least squares (OLS), quantile regressions (QR), and the nonparametric B-splines regression model. The results show a negative, asymmetric and nonlinear contemporary relationship between the two series, that the effects of negative shocks in volatility are more obvious than positive shocks, and, excitingly, the association has no homogeneous behavior across the various quantiles. Utilizing nonparametric quantile models, Fousekis [46] reveals that the association between oil price returns and OVX is contemporaneous, negative, and asymmetric, and indicates the presence of an inverted U-shaped dependence between the two measures, indicating that the pricing of implied volatility is higher for large fluctuations than for small ones, and are lighter for large positive variations than for large negative ones. Lin and Tsai [40] examine the long-run dynamics between oil prices and OVX. They reveal that increasing OVX exhibits a larger negative influence on oil prices than declining OVX, indicating the existence of a long-run asymmetric cointegrating relationship between them. It is worth mentioning that this result of asymmetry is also recognized in previous findings [41–57]. Furthermore, Shaikh [44] uses neural network and quantile approaches and suggests that crude oil prices are aligned with OVX. They find an asymmetric relationship and show evidence that the implied volatility is likely to be calm during global financial crises and increases after the crisis periods. Echaust and Just [42] study the tail dependence behavior of WTI oil returns and OVX changes. The

results suggest that the strongest tail dependence of negative oil price shocks and OVX changes happens during the pandemic crisis. They establish the ability of the OVX index to be a sentiment indicator for the crude oil market. Nevertheless, they fail to ascertain its capability to ameliorate value-at-risk estimates. Li et al. [43] explore the characteristics of the cross-correlations between the crude oil market and OVX. The findings reveal that the cross-correlated compartments of smaller changes are persistent, although large changes are anti-persistent between crude oil and OVX. Furthermore, the results confirm that oil price variations and OVX change in a positive direction in the short-term, although they change in the inverse direction in the long-term.

More recently, Raggad [58] applies the Cross-Quantilogram approach to explore whether the OVX can reliably predict WTI returns, and finds that the information content of OVX plays a role in forecasting WTI returns once it is in the higher conditional quantile, but no evidence of predictability is uncovered once the OVX is at the low to medium quantile levels.

As we can see from the above review, the existing literature does not examine the directional predictability patterns between oil returns and oil implied volatility, based on a quantile-based methodology that can potentially enrich our understanding of the sign, magnitude, duration, and asymmetric Granger causal interactions between oil returns and oil implied volatility across upper, middle, and lower quartiles. This is where we aim to contribute.

3. Methodology

The first sub-section briefly introduces the quantile autoregressive (QAR) unit root tests of Koenker and Xiao [59] and Galvao [47]. The second sub-section presents the Granger causality test in the quantiles of Troster [48]. The third sub-section describes the nonparametric cross-quantilogram approach of Han et al. [49].

3.1. Quantile Unit Root Test

Researchers give attention to quantile autoregressive (QAR) unit root tests when examining the stationarity properties of time series. A major reason for the use of this kind of test is its ability to investigate the stationarity property of data across the quantiles of the conditional distribution beyond the limitation of the conditional mean [60]. This test is of immense importance for accurately identifying the dynamic behavior and distributed characteristics of the time series data [61]. QAR unit root tests were introduced by Koenker and Xiao [59] and later generalized by Galvao [47], who explicitly incorporated covariates and a linear time trend into the QAR specification.

To formalize the idea empirically, suppose that the time series process X_t is strictly stationary and let $\Omega_t = (X_{t-1}, \dots, X_{t-s})' \in \mathbb{R}^d$ be an information set based on the history of Y_t . Let us denote by $F_X(\cdot \mid \Omega_t^X)$ the conditional distribution function of X_t given Ω_t^X , so the QAR unit root test is specified by a quantile linear regression model. Specifically, the QAR model is described as:

$$Q_\tau^X(X_t \mid \Omega_t^X) = \lambda_1(\tau) + \lambda_2(\tau)t + \beta(\tau)X_{t-1} + \sum_{j=1}^p \beta_j(\tau)\Delta X_{t-j} + F_u^{-1}(\tau) \quad (1)$$

where $Q_\tau^X(\cdot \mid \Omega_t^X)$ is the τ -quantile of $F_X(\cdot \mid \Omega_t^X)$, $\lambda_1(\tau)$ defines the drift term, t designates the linear time trend, $\beta(\tau)$ represents the persistence measure, and F_u^{-1} denotes the inverse conditional distribution function of the errors based on various quantiles τ , $\tau \in \Gamma \subset [0,1]$.

By estimating Equation (1) for various quantiles, we obtain the estimation of the persistence measure $\hat{\beta}$ corresponding to each quantile of the conditional distribution Y_t . The null hypothesis of the QAR test is expressed as: $H_0: \beta(\tau) = 1$, and its respective t -test is calculated through the t -statistic suggested by Koenker and Xiao [59] and Galvao [47] for the entire range of quantiles $\tau \in \Gamma$.

3.2. Granger Causality in Quantiles

As noted, the test of Troster [48] has the merit of taking into account potential nonlinear causal relations in the conditional quantiles of the return distribution. It is sufficiently flexible to test for Granger causality in specific regions of the distribution, such as the center or tails (left or right).

To formally present the test, let $\{Y_t, Z_t, t \in Z\}$ be a jointly stationary and ergodic time series defined in some probability space (Ω, A, P) and $Y_t \in \mathbb{R}$ be a dependent variable; and let $J_t \in \mathbb{R}^d, d = s + q$, be an explanatory vector, given by: $J_t \equiv (J_t^Y, J_t^Z)'$, where $J_t^Y := \{Y_{t-1}, \dots, Y_{t-s}\}' \in \mathbb{R}^s$ and $J_t^Z := \{Z_{t-1}, \dots, Z_{t-q}\}' \in \mathbb{R}^q$.

The null hypothesis for the Granger causality test assumes that Z_t does not Granger-cause Y_t and is given by:

$$H_0^{Z \nrightarrow Y} : F_Y(y \setminus J_t^Y, J_t^Z) = F_Y(y \setminus J_t^Y) \text{ for all } y \in \mathbb{R}, \tag{2}$$

where $F_Y(\cdot \setminus J_t^Y, J_t^Z)$ and $F_Y(\cdot \setminus J_t^Y)$ designate the conditional distribution function of Y_t given (J_t^Y, J_t^Z) and J_t^Y , respectively. The null hypothesis defined by Equation (2) is called Granger non-causality in distribution.

Given the difficulty in estimating the conditional distribution, the formulation defined by Equation (2) is limited to the test for Granger non-causality in mean, which is barely a necessary condition for the expression given by Equation (3) [48]. It follows that Z_t does not Granger-cause Y_t in mean if:

$$E(Y_t \setminus J_t^Y, J_t^Z) = E(Y_t \setminus J_t^Y) \text{ for all } y \in \mathbb{R} \tag{3}$$

where $E(Y_t \setminus J_t^Y, J_t^Z)$ and $E(Y_t \setminus J_t^Y)$ represent the means of $F_Y(\cdot \setminus J_t^Y, J_t^Z)$ and $F_Y(\cdot \setminus J_t^Y)$, respectively.

As noted by Troster [48], the preceding specifications have two major drawbacks. Firstly, the uniform causality in mean fails to accommodate potential links in the extreme conditional quantiles of the distribution. Secondly, the null hypothesis described in Equation (3) tells us nothing of the “level of the causality” in the case of rejecting the hypothesis. To overcome these two limitations, Troster [48] proposes Granger non-causality in conditional quantiles.

By substituting $F_Y(\cdot \setminus J_t^Y, J_t^Z)$ and $F_Y(y \setminus J_t^Y)$ by their τ -quantiles, noted by $Q_\tau^{Y,Z}(\cdot \setminus J_t^Y, J_t^Z)$ and $Q_\tau^Y(y \setminus J_t^Y)$, respectively, in Equation (2), the following expression can be obtained:

$$H_0^{QC, Z \nrightarrow Y} : Q_\tau^{Y,Z}(y \setminus J_t^Y, J_t^Z) = Q_\tau^Y(y \setminus J_t^Y), \text{ a.s. for all } \tau \in \Gamma, \tag{4}$$

where Γ is a compact set such that $\Gamma \subset [0,1]$, and the conditional τ -quantiles of Y_t fulfil the subsequent constraints (conditions):

$$Pr\{Y_t \leq Q_\tau^Y(y \setminus J_t^Y) \setminus J_t^Y\} = \tau \text{ for all } \tau \in \Gamma$$

$$Pr\{Y_t \leq Q_\tau^{Y,Z}(y \setminus J_t^Y, J_t^Z) \setminus J_t^Y, J_t^Z\} = \tau \text{ for all } \tau \in \Gamma$$

With an explanatory vector J_t , we get $Pr\{Y_t \leq Q_\tau^Y(y \setminus J_t^Y) \setminus J_t^Y\} = E\{1[Y_t \leq Q_\tau^Y(y \setminus J_t^Y) \setminus J_t^Y]\}$, where $1[Y_t \leq y]$ denotes an indicator function of the event that Y is less than or equal to y . Therefore, Equation (4) can be written in its equivalent form:

$$E\{1[Y_t \leq Q_\tau^{Y,Z}(y \setminus J_t^Y, J_t^Z) \setminus J_t^Y, J_t^Z]\} = E\{1[Y_t \leq Q_\tau^Y(y \setminus J_t^Y) \setminus J_t^Y]\}, \text{ a.s. for all } \tau \in \Gamma \tag{5}$$

where the left-hand side of Equation (5) defines the τ -quantile of $F_Y(\cdot \setminus J_t^Y, J_t^Z)$ by definition. Following Troster [48], a parametric model is required for the estimation of the τ -th quantile of $F_Y(\cdot \setminus J_t^Y)$. To this end, suppose that $Q_Y(\cdot \setminus J_t^Y)$ is appropriately modelled by a parametric quantile specification

$s(\cdot, \varphi(\tau))$, which belongs to a set of functions $S = \{s(\cdot, \varphi(\tau)) \setminus \varphi(\cdot) : \tau \rightarrow \varphi(\tau) \in \Phi \subset \mathbb{R}^p, \text{ for } \tau \in \Gamma \subset [0, 1]\}$.

Next, under the null hypothesis given by Equation (5), the τ -conditional quantile, $Q_Y(\cdot \setminus J_t^Y)$, is appropriately modelled by a parametric quantile specification $s(J_t^Y, \varphi_0(\tau))$ defined on the subset information J_t^Y . It follows that the null hypothesis of absence of Granger causality is reformulated as follows:

$$H_0^{QC, Z \nrightarrow Y} : E\left\{1\left[Y_t \leq s\left(J_t^Y, \varphi_0(\tau)\right) \setminus J_t^Y, J_t^Z\right]\right\} = \tau, \text{ a.s. for all } \tau \in \Gamma, \tag{6}$$

Versus

$$H_A^{QC, Z \nrightarrow Y} : E\left\{1\left[Y_t \leq s\left(J_t^Y, \varphi_0(\tau)\right) \setminus J_t^Y, J_t^Z\right]\right\} \neq \tau, \text{ a.s. for all } \tau \in \Gamma, \tag{7}$$

where $s(J_t^Y, \varphi_0(\tau))$ appropriately defines the true conditional quantile $Q_Y(\cdot \setminus I_t^Y)$, for all $\tau \in \Gamma$. Equation (6) can be reformulated as $H_0^{QC, Z \nrightarrow Y} : E\{1[(Y_t - m(I_t^Y, \varphi_0(\tau))) \leq 0 - \tau] \setminus I_t^Y, I_t^Z\} = 0$, for all $\tau \in \Gamma$. Furthermore, the null hypothesis of Equation (6) can be described by a sequence of unconditional moment restrictions such as:

$$E\left\{1\left[(Y_t - s\left(I_t^Y, \varphi_0(\tau)\right)) \leq 0 - \tau\right] \exp(i\omega' I_t)\right\} = 0, \text{ for all } \tau \in \Gamma \tag{8}$$

where $\exp(i\omega' I_t) := \exp(i\omega_1(Y_{t-1}Z_{t-1})' + \dots + i\omega_r(Y_{t-r}Z_{t-r})')$ represents a weighting function for all $\omega \in \mathbb{R}^r$ with $r \leq d$, and $i = \sqrt{-1}$ is the imaginary root. Hence, a parametric test statistic can be formulated as the sample analogue of this expression $E\{1[(Y_t - s(I_t^Y, \varphi_0(\tau))) \leq 0 - \tau] \exp(i\omega' I_t)\}$:

$$v_T(\omega, \tau) = \frac{1}{\sqrt{T}} \sum_{t=1}^T \left\{1\left[(Y_t - s\left(I_t^Y, \varphi_T(\tau)\right)) \leq 0 - \tau\right] \exp(i\omega' I_t)\right\} \tag{9}$$

where φ_T is a \sqrt{T} -consistent estimator of $\varphi_0(\tau)$, for all $\tau \in \Gamma$. Then, the following test statistic suggested by Troster [48] can be deduced:

$$z_T := \iint_{TW} |v_T(\omega, \tau)|^2 dF_\omega(\omega) dF_T(\tau) \tag{10}$$

where the function $F_\omega(\cdot)$ designates the conditional distribution of a d-variate standard normal vector, $F_T(\cdot)$ is a uniform discrete distribution defined on the set of T in n equally spaced random points, $T_n = \{\tau_j\}_{j=1}^n$, and $\omega \in \mathbb{R}^d$ is the vector of weights obtained from a standard normal distribution. The expression of Equation (10) can be assessed by its sample equivalent. Consider a $T \times n$ matrix with components $\psi_{ij} = \Psi_{\tau_j}(Y_i - s(I_i^Y, \varphi_T(\tau_j)))$, where $\Psi_{\tau_j}(\cdot)$ is the function $\Psi_{\tau_j}(\varepsilon) := 1(\varepsilon \leq 0) - \tau_j$. The test is therefore based on the statistic:

$$z_T := \frac{1}{Tn} \sum_{j=1}^n \left| \psi_j' W \psi_j \right| \tag{11}$$

where W is the $n \times n$ matrix with components $w_{ts} = \exp(-0.5(J_t - J_s)^2)$ and ψ_j' designates the j-th column of Ψ . The rejection of the null hypothesis of the test is conditioned by observing large values of z_T in Equation (11).

Following the pioneering work of Troster [48], the subsampling procedure is applied to compute critical values for z_T in Equation (11). The procedure therefore consists of computing z_T for the whole subsample, and the p-values are deduced from the average value of the B subsamples test statistics.

Notably, the subsample is selected of size $b = \lfloor kT^{2/5} \rfloor$, where $\lfloor \cdot \rfloor$ stands for the integer part of a number, and k is a constant term [62].

To obtain the z_T test, as given in Equation (11), we follow Troster [48] and choose three QAR specifications $s(\cdot)$, for different quantiles of order τ , $\tau \in \Gamma \subset [0, 1]$, under the null hypothesis of absence of Granger causality in Equation (8) as:

$$QAR1 : s^1\left(J_t^Y, \varphi(\tau)\right) = \lambda_1(\tau) + \lambda_2(\tau)Y_{t-1} + \beta_t F_u^{-1}(\tau) \tag{12}$$

$$QAR2 : s^2\left(J_t^Y, \varphi(\tau)\right) = \lambda_1(\tau) + \lambda_2(\tau)Y_{t-1} + \lambda_3(\tau)Y_{t-2} + \beta_t F_u^{-1}(\tau) \tag{13}$$

$$QAR3 : s^3 \left(J_t^Y, \varphi(\tau) \right) = \lambda_1(\tau) + \lambda_2(\tau)Y_{t-1} + \lambda_3(\tau)Y_{t-2} + \lambda_4(\tau)Y_{t-3} + \beta_t F_u^{-1}(\tau) \tag{14}$$

where the parameters $\varphi(\tau) = (\lambda_1(\tau), \lambda_2(\tau), \lambda_3(\tau), \lambda_4(\tau), \beta_t)'$ are estimated by a maximum likelihood method, and F_u^{-1} denotes the inverse of a standard normal distribution.

3.3. The Cross-Quantilogram

We investigate the directional quantile dependence and spillover effect between WTI returns and OVX changes across quantiles by utilizing the cross-quantilogram method of Han et al. [49]. This method has various attractive features. Firstly, it captures the correlation and causal dependence between the two variables, irrespective of the distribution region. Secondly, it is free of any distributional assumptions regarding the variables under study to test causality. Thirdly, it allows us to deal with long lags in the Granger causality test.

Formally, the method is presented as follows. For any two-dimensional strictly stationary time series $\{x_{i,t}, t \in Z\}$, $i = 1, 2$, we denote by $F_i(\cdot)$ the cumulative distribution of $x_{i,t}$ with density functions $f_i(\cdot)$ for $i = 1, 2$. The respective quantile of the series $x_{i,t}$ is given by $q_i(\alpha_i) = \inf\{u : F_i(u) \geq \alpha_i\}$ for $\alpha_i \in [0, 1]$. In a bivariate setting, the quantiles of order $\alpha = (\alpha_1, \alpha_2)'$ are given by $(q_1(\alpha_1), q_2(\alpha_2))'$. To detect the quantile dependence between the two series, the cross-quantilogram, CQ, for the α -quantile with k lags can be found by applying the formula:

$$\rho_k(\alpha) = \frac{E[\Psi_{\alpha_1}(x_{1,t} - q_1(\alpha_1))\Psi_{\alpha_2}(x_{2,t-k} - q_{2,t-k}(\alpha_2))]}{\sqrt{E[\Psi_{\alpha_1}^2(x_{1,t} - q_1(\alpha_1))]} \sqrt{E[\Psi_{\alpha_2}^2(x_{2,t-k} - q_{2,t-k}(\alpha_2))]}} \tag{15}$$

For $k = 0, \pm 1, \pm 2, \dots$, where $\Psi_\alpha(u) \equiv 1[u < 0] - \alpha$, the term $1[\cdot]$ indicates the indicator function, while $1[x_{i,t} \leq q_i(\alpha_i)]$ is recognized as the quantile hit or quantile exceedance process. It follows that the sample form of CQ, based on observed data, is defined as:

$$\hat{\rho}_\alpha(k) = \frac{\sum_{t=k+1}^T [\Psi_{\alpha_1}(x_{1,t} - \hat{q}_1(\alpha_1))\Psi_{\alpha_2}(x_{2,t-k} - \hat{q}_{2,t-k}(\alpha_2))]}{\sqrt{\sum_{t=k+1}^T [\Psi_{\alpha_1}^2(x_{1,t} - \hat{q}_1(\alpha_1))]} \sqrt{\sum_{t=k+1}^T [\Psi_{\alpha_2}^2(x_{2,t-k} - \hat{q}_{2,t-k}(\alpha_2))]}} \tag{16}$$

Note that the $\hat{q}_i(\alpha_i)$ parameter in Equation (16) designates the unconditional sample quantile of $x_{i,t}$, as specified by Han et al. [49]. Furthermore, Han et al. [49] suggest a quantile form of the Ljung–Box–Pierce test statistic with the null hypothesis $H_0: \hat{\rho}_\alpha(k) = 0$ for all $k \in 1, \dots, p$. $H_1: \hat{\rho}_\alpha(k) \neq 0$ for all $k \in 1, \dots, p$:

$$\hat{Q}_\alpha^{(p)} = \frac{T(T+1) \sum_{k=1}^p \hat{\rho}_\alpha^2(k)}{T-k} \tag{17}$$

where $\hat{Q}_\alpha^{(p)}$ represents the portmanteau test of directional predictability from one time series to another corresponding to p lags and quantile pair $\alpha = (\alpha_1, \alpha_2)$. For the construction of confidence intervals for the cross-quantilogram, Han et al. [49] suggest using the stationary bootstrap inference procedure and a self-normalized approach.

4. Data and Preliminary Analysis

4.1. Data Description

We use WTI crude oil prices and OVX. WTI is a global benchmark for crude oil prices in the US. The sample period spans 10 May 2007 to 17 April 2020 (yielding 3376 daily observations), based on the availability of OVX data sourced from CBOE. Data on crude oil prices are collected from the online database of the US Energy Information Administration (EIA). Our empirical analysis employs daily WTI and OVX returns computed as log-difference $R_t = 100 * \ln(\frac{S_t}{S_{t-1}})$; where $S_t = WTI$, or OVX. Figure 1 shows the time evolution of the daily levels and returns series over the period of investigation, and Table 1 gives the summary statistics of the daily return series.

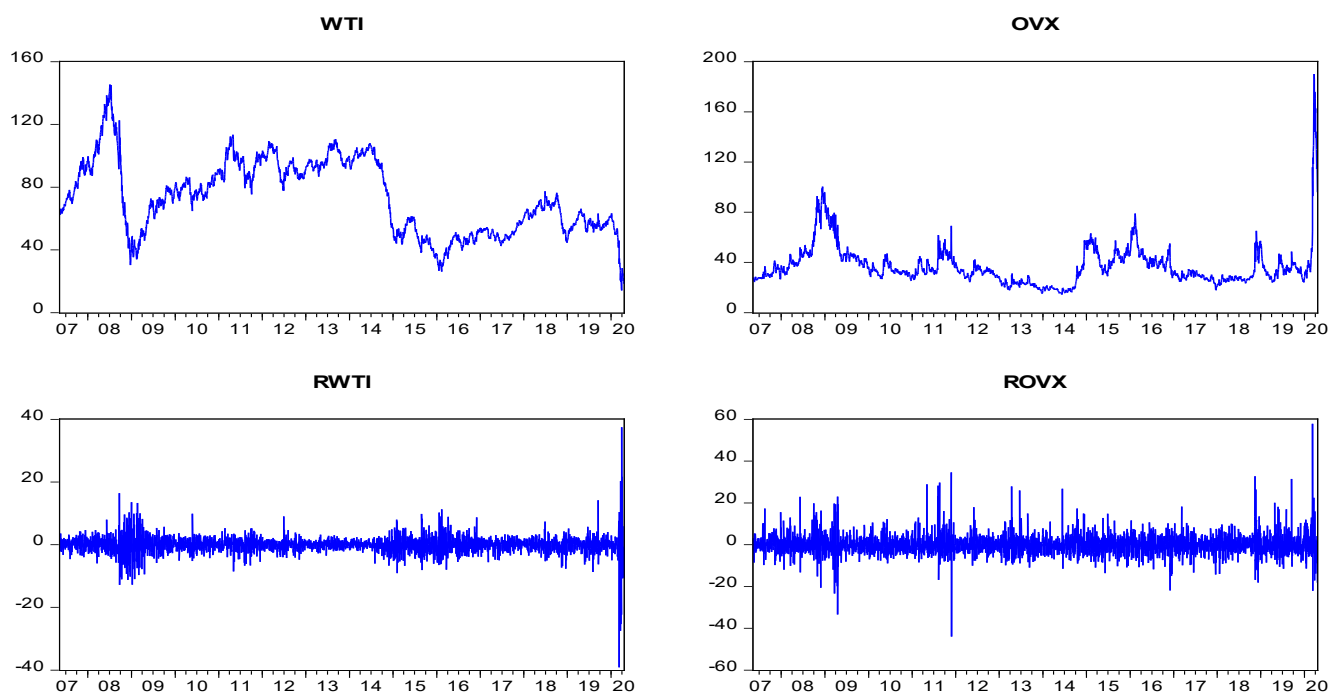


Figure 1. Evolution of daily levels and returns of WTI crude oil and OVX.

Table 1. Summary statistics of returns series for WTI and OVX.

	WTI	OVX
Mean	−0.036	0.037
Median	0.053	−0.27
Maximum	37.474	57.821
Minimum	−39.087	−43.991
Std. Dev.	2.747	4.938
Skewness	−0.402	1.057
Kurtosis	35.974	16.026
Jarque-Bera	153,031.3 ***	24,497.87 ***
Ljung-Box	85.20 ***	51.134 ***
Observations	3376	3376
Correlation		−0.325 ***

Notes: The sample period is 10 May 2007 to 17 April 2020. *** denotes statistical significance at the 1% level.

As shown in Figure 1, both level and return series exhibit various significant fluctuations that usually concur with major geopolitical, fundamental, or economic events that affect the oil market, such as the 2008 Global Financial Crisis (GFC), the 2009–2012 euro-zone debt crisis, the Libyan crisis of 2011, the 2014–2016 Oil Price Slump, and the oil market turmoil related to the COVID-19 health crisis. The descriptive statistics of daily returns shown in Table 1 indicate that neither WTI returns nor OVX returns are normally distributed, as shown by the excess kurtosis and evidence that the return distributions are leptokurtic with asymmetric tails. The Jarque-Bera test confirms the rejection of the null hypothesis of normality for both return series. This result is validated by the Q-Q normal plot of the series given in Figure 2, because the quantile points deviate from the reference line.

While the OVX returns have a positive skewness, the WTI returns exhibit negative skewness, demonstrating a fatter tail on the left side (losses) of the distribution. The correlation between the two variables is significantly negative (−0.325). To test for serial correlation, we use the Ljung-Box statistic. The result reveals that the null hypothesis of no autocorrelation up to 20 lags is rejected and proves the existence of conditional heteroskedasticity in the dynamics of both series. As a reaction to the influx of new information, the market adjusts the volatility forecast and, accordingly, options prices.

It is worth noting that, as a part of our preliminary investigation, we assess the presence of non-linearity by performing the Brock–Dechert–Scheinkman (BDS) test of Brock et al. [63] on the residuals of the oil and OVX returns equations in the vector autoregressive (VAR) (1) model. As

Table 2 shows, the null hypothesis of i.i.d. residuals is rejected at different embedding dimensions (m), providing evidence of non-linearity in the data.

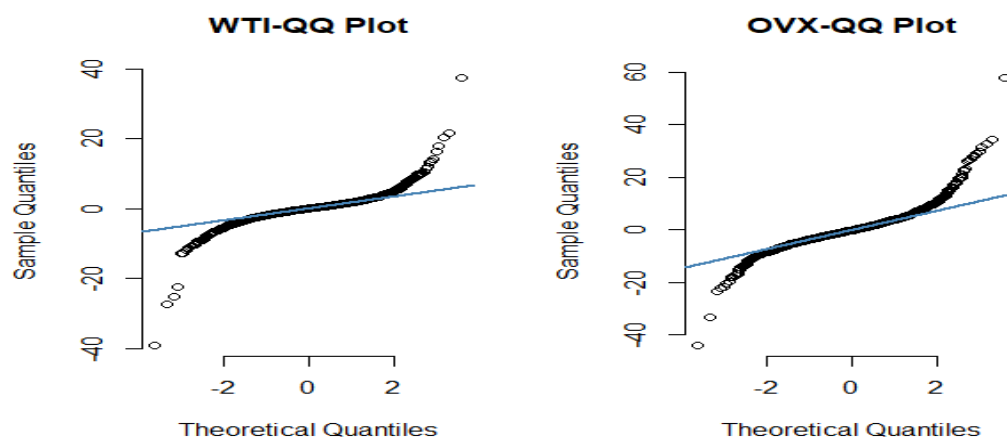


Figure 2. Q-Q plots of the series.

Table 2. Results of Brock–Dechert–Scheinkma (BDS) statistics from VAR residuals.

m	WTI	OVX
2	0.029 ***	0.018 ***
3	0.056 ***	0.033 ***
4	0.074 ***	0.04 ***
5	0.083 ***	0.045 ***
6	0.087 ***	0.046 ***
2	0.029 ***	0.018 ***

Note: The values denote the BDS test built on the residuals of WTI and OVX returns in a VAR. m represents the embedding dimension of the BDS test. *** signifies rejection of the null of residuals being i.i.d. at the 1% significance level.

We also check for the existence of multiple structural breaks by conducting the methodology developed by Bai and Perron [64]. Unreported results provide evidence of non-linearity and the presence of at least one structural break in both WTI and OVX return series.

4.2. Unit Root Testing

We begin by examining the stationarity properties of our time series. This step is a key requirement for performing our statistical methodology. Using three familiar unit root tests, specifically the Augmented Dickey and Fuller [65] (ADF), the Phillips and Perron [66] (PP), and the Zivot and Andrews [67] (ZA) tests, Table 3 shows that the return series are stationary at the 1% significance level.

Table 3. Results for conventional unit root tests for the two series.

	OVX	WTI
ADF Test	−59.922 ***	−62.137 ***
PP Test	−60.180 ***	−62.107 ***
ZA Test	−36.084 ***	−29.688 ***

Note: ***, **, and * indicate the rejection of the null hypothesis at the 1% 5% and 10% significance levels, respectively.

As a part of our full quantile-based statistical methodology, we also include in our analysis the QAR unit root test to check whether or not the unit root results persist across the quantiles of the conditional distribution, not only at the conditional mean. As noted by Koenker and Xiao [59], this kind of test has higher power than conventional unit root tests. Furthermore, the quantile-based unit root test outperforms conventional unit root tests in case of a deviation from the hypothesis of Gaussian residuals. The results of the quantile unit root test are given in Table 4, which shows the persistence measure estimates as well as the t-statistics at the 5% significance levels, under the null hypothesis $H_0: \beta(\tau) = 1$, for various quantiles $\tau \in [0.05, 0.95]$.

Table 4. Quantile autoregression unit root test results.

τ	WTI			OVX		
	$\beta(\tau)$	T-Stat	CV	$\beta(\tau)$	T-Stat	CV
0.05	0.047	−10.595	−3.37	−0.154	−23.545	−2.31
0.1	0.031	−19.564	−3.35	−0.111	−42.006	−2.31
0.15	0.049	−25.391	−3.293	−0.092	−48.172	−2.31
0.2	0.075	−29.558	−3.236	−0.055	−55.28	−2.313
0.25	0.065	−34.652	−3.236	−0.047	−60.029	−2.385
0.3	0.038	−38.02	−3.208	−0.039	−62.469	−2.53
0.35	0.023	−43.397	−3.195	−0.041	−63.142	−2.588
0.4	0.015	−47.051	−3.136	−0.03	−65.601	−2.65
0.45	0.011	−48.649	−3.073	−0.029	−67.283	−2.644
0.5	−0.002	−51.437	−3.07	−0.024	−65.054	−2.704
0.55	−0.012	−53.711	−3.066	−0.02	−62.884	−2.742
0.6	−0.01	−52.972	−3.01	0.007	−59.946	−2.854
0.65	−0.023	−51.49	−2.964	0.016	−54.166	−2.895
0.7	−0.044	−49.292	−2.884	0.018	−49.539	−2.888
0.75	−0.067	−45.158	−2.764	0.038	−45.41	−2.902
0.8	−0.092	−39.279	−2.575	0.067	−41.718	−2.901
0.85	−0.121	−34.714	−2.491	0.052	−38.062	−2.914
0.9	−0.168	−28.373	−2.31	0.088	−22.758	−3.036
0.95	−0.149	−13.036	−2.31	0.075	−7.644	−3.154

Notes: This table displays the outcomes of the quantile unit root test for the grid of 19 quantiles, $\tau = 0.05, \dots, 0.95$. The procedure consists of testing the null hypothesis of the unit root $H_0: \beta(\tau) = 1$. The null hypothesis of unit roots is rejected at quantile τ when the test-statistics are less than 5% the critical value (CV).

Both return series are stationary, irrespective of the level of significance, for all the considered quantiles of the conditional distribution. These findings support the previous results obtained with the conventional unit root tests (Table 3). Having this in hand, we proceed to the implementation of the quantile-based methodology.

4.3. Testing for Cointegration

We conduct the linear cointegration test of Johansen [68,69] and the quantile cointegration test suggested by Xiao [70] to check whether the series are cointegrated. Panel A of Table 5 indicates that there exists a linear cointegration between the series at the 5% significance level. Panel B, the results of the quantile cointegration test proposed by Xiao [70], shows evidence of a significantly non-linear cointegration relationship between the quantiles of both series at any level of significance, indicating that the cointegration link between the variables changes over the distribution.

Table 5. Results of linear and quantile cointegration tests.

<i>Panel A: Johansen Linear Cointegration Test</i>					
		Trace statistic H0: rank = 0 (15.41)	Max. eigenvalue statistic H0: rank = 0 (14.07)		
WTI-OVX		20.202 (**)	18.992 (**)		
<i>Panel B: Quantile Cointegration Test</i>					
model	coefficient	$\text{Sup}_\tau \left \hat{V}_n(\tau) \right $	critical values		
			1%	5%	10%
WTI versus OVX	beta	7406.825 (***)	250.470	141.558	115.485
	gamma	935.6308 (***)	20.814	13.542	9.543

Notes: Panel A shows the result for the test of Johansen [68,69] for oil price and OVX, taken in natural logarithm form. Numbers in parentheses next to H0: rank = 0 are the 5% critical values of the corresponding test statistic. Panel B shows the test statistic of the quantile cointegration model between the considered variables computed using an equally spaced grid of 19 quantiles [0.05; 0.95]. *** and ** denote the rejection of the null hypothesis at the 1% and 5% significance level, respectively.

Overall, the non-normality of the unconditional distribution, the non-linearity, and the presence of structural breaks in our data provide preliminary support for the use of the causality in quantiles test and the cross-quantilogram approach.

5. Empirical Results

5.1. Granger Causality Test Results

To explore the Granger causal relationship between WTI returns and OVX returns, we begin by conducting the standard test of Granger causality, for the purpose of comparison. The results of the Granger causality test between WTI and OVX, with three lag-lengths, $k = 1, 2, 3$, are given in Table 6. They show that the null of no Granger causality existing from WTI returns to OVX changes, cannot be rejected at any level of significance. However, OVX returns are found to Granger-cause in mean WTI returns at the 5% significance level. Notably, these results should be taken with caution because the standard test of Granger causality does not account for potential non-linearity.

Table 6. p -values of the standard test of Granger causality (in mean).

	Number of Lags		
	1	2	3
H_0 : WTI does not Granger-cause OVX	0.341	0.35	0.441
H_0 : OVX does not Granger-cause WTI	0.00 **	0.001 **	0.002 **

Notes: ** denotes statistical significance at the 5% level.

After verifying the stationarity of our data, we are justified in the application of the parametric test of Troster [48] to examine the Granger causality in quantiles. While the standard Granger causality test shows evidence of a mean unidirectional causal relationship running from OVX changes to WTI returns, it is important to evaluate the validity of such a relationship at each of the quantiles considered. To this end, we follow Troster [48] and estimate three different QAR models, given by Equations (11)–(13), for each dependent variable in the z_T test, given by Equation (11). Following Sakov and Bickel [62], a subsample is chosen of size $b = \lfloor kn^{2/5} \rfloor$, where $\lfloor \cdot \rfloor$ corresponds to the integer part of a number, the constant parameter is given by $k = 5$, and $n = 3373$ is the sample size. The subsequent subsample size is $b = 129$, but the unreported results show that the findings are not very sensitive to other choices of subsample size.

With this quantile approach test, we can distinguish between causality affecting the various portions of the conditional distribution (i.e., lower, median, or upper quantiles). Table 7 shows the subsample p -values of the z_T test defined by Equation (11). WTI returns oil prices Granger-cause OVX returns at the 1% significance level, for all quantiles considered, except some quantiles in the middle part of the distribution (i.e., 0.4 and 0.45). For the reverse direction, there is evidence of Granger causality from OVX returns to WTI returns. However, we fail to confirm evidence for Granger causality either at the extreme quantiles or in the near centrally located quantiles of the distribution. Notably, these results are not sensitive to lag-length defining the QAR specification, under the null hypothesis of no Granger causality. These findings are partially in line with the result of Lin et al. [71], who report that oil prices have a bi-directional relation with OVX. Similarly, in a different application, Liu et al. [17] find a significant bi-directional implied volatility transmission between oil and US stock markets.

While the test of Troster [48] provides some insight into the causal relationships in conditional quantiles, it has one major drawback, which is common for parametric approaches, which is that it might be subject to ambiguous results owing to misspecification and consequently may lose its full ability to capture the true causal relationships between the return series. Additionally, the test of Troster [48] does not indicate the extent or sign of the relationship for the variables in question. Subsequently, to overcome these potential problems and for reasons of comparability, we apply the nonparametric cross-quantilogram approach of Han et al. [49].

5.2. Cross-Quantilogram Analysis

The results of the CQ are graphic, and in each plot we report the sample cross-quantilograms for lag $k = 1, 2, \dots, 30$, in conjunction with the 95% bootstrapped confidence intervals for no directional predictability with 1000 bootstrapped replicates, distinguished by red-dashed lines. The findings for the relationship between WTI and OVX returns are given in Figures 3–6, when both markets are in the same quantiles, i.e., for the grid of 19 quantiles $\tau = [0.05; 0.95]$, and in Figures 7–12 when both markets are in opposite quantiles. Note that if $\rho_k(\alpha) = 0$, there is no dependence or directional predictability

from an event $\{x_{2,t-k} \leq q_{2,t-k}(\tau_2) : k = 1, \dots, p\}$ to an event $\{x_{1,t-k} \leq q_{1,t-k}(\tau_1) : k = 1, \dots, p\}$. In contrast, if $\rho_k(\alpha) \neq 0$, there is a quantile dependence or directional predictability between the two events. In our framework, the lead/lag parameter k , defined in terms of days, governs the delay in the predictability from one return time series to another.

Table 7. Granger causality in quantiles: subsample p -values.

Quantiles	WTI to OVX			OVX to WTI		
	Number of Lags			Number of Lags		
	1	2	3	1	2	3
0.05	0.0003	0.0003	0.0003	0.0003	0.0003	0.0003
0.1	0.0003	0.0003	0.0003	0.0003	0.0003	0.0003
0.15	0.0003	0.0003	0.0003	0.0003	0.0003	0.0003
0.2	0.0003	0.0003	0.0003	0.0003	0.0003	0.0003
0.25	0.0003	0.0003	0.0003	0.0003	0.0003	0.0003
0.3	0.0003	0.0003	0.0003	0.0003	0.0003	0.0003
0.35	0.0003	0.0003	0.0003	0.0151	0.0031	0.0031
0.4	0.1624	0.1445	0.3552	0.3417	0.7967	0.7699
0.45	0.2597	0.3121	0.1673	0.0034	0.0111	0.0089
0.5	0.0003	0.0003	0.0003	0.0003	0.0003	0.0003
0.55	0.0003	0.0003	0.0003	0.0003	0.0003	0.0003
0.6	0.0003	0.0003	0.0003	0.0003	0.0003	0.0003
0.65	0.0003	0.0003	0.0003	0.0003	0.0003	0.0003
0.7	0.0003	0.0003	0.0003	0.0003	0.0003	0.0003
0.75	0.0003	0.0003	0.0003	0.0003	0.0003	0.0003
0.8	0.0003	0.0003	0.0003	0.0003	0.0003	0.0003
0.85	0.0003	0.0003	0.0003	0.0003	0.0003	0.0003
0.9	0.0003	0.0003	0.0003	0.0003	0.0003	0.0003
0.95	0.0086	0.0062	0.0123	0.9356	1	1

Note: The values in bold are the p -values indicating the rejection of the null hypothesis of no quantile Granger causality at the 1% significance level.

5.2.1. Results When Both Return Series Are in the Same Quantiles

Figures 3 and 4 show the cross-quantilogram and Box–Ljung test statistics for the directional predictability from WTI returns to OVX returns. The results show that WTI returns have a positive and significant effect on OVX returns when both are at their lower quantiles (less than 0.4). However, in general, this OVX quantile reliance on WTI is dispelled for larger lags, with a few non-substantial exceptions for some lags, suggesting that the relationship weakens over time. On the other hand, there is no sufficient evidence of dependence between the two return series when they are at intermediate to higher quantiles, except for some quantiles such as 0.45 and 0.5. We note that the quantile dependence is asymmetric as the negative spillover is stronger than the positive spillover.

In the case of the spillover from OVX to WTI, as shown in Figures 5 and 6, OVX exhibits a positive and significant impact on WTI when both return series are at the upper quantiles. We, however, do not see any sufficient evidence of causality when the two return series are in lower to intermediate quantiles. These findings indicate that oil prices surge as OVX, which includes investor sentiment or a fear component, surges. In other words, when there is increasing uncertainty in the crude oil market, as reflected by an increasing OVX, both crude oil prices and OVX tend to leap upwards together. This result is in line with previous studies such as Jagerson (2008), who postulates that OVX can forecast oil prices, and Aboura & Chevallier [38], who establish that a surge in the oil price is followed by a surge in volatility. The results support the findings of Liu et al. [21], who show that WTI returns are more sensitive to OVX upsurges than OVX declines. Equally, we note that the quantile dependence is asymmetric as the spillover between right tails is higher than the spillover between left tails.

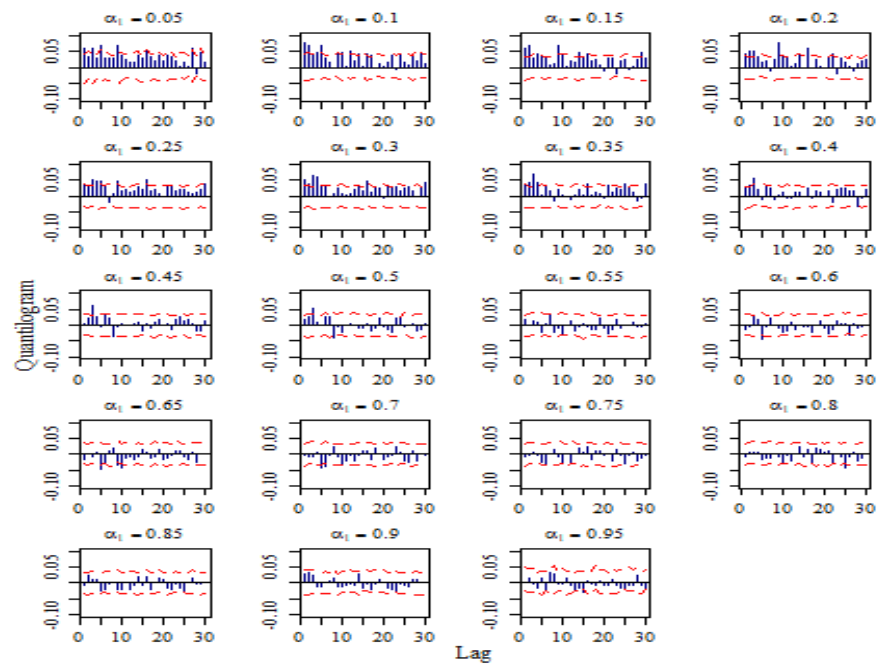


Figure 3. Sample cross-quantilograms, to capture directional predictability from WTI to OVX, when both return series are in the same quantiles. Results with lag $k = 1, 2, \dots, 30$. The dashed lines denote the 95% bootstrapped confidence intervals.

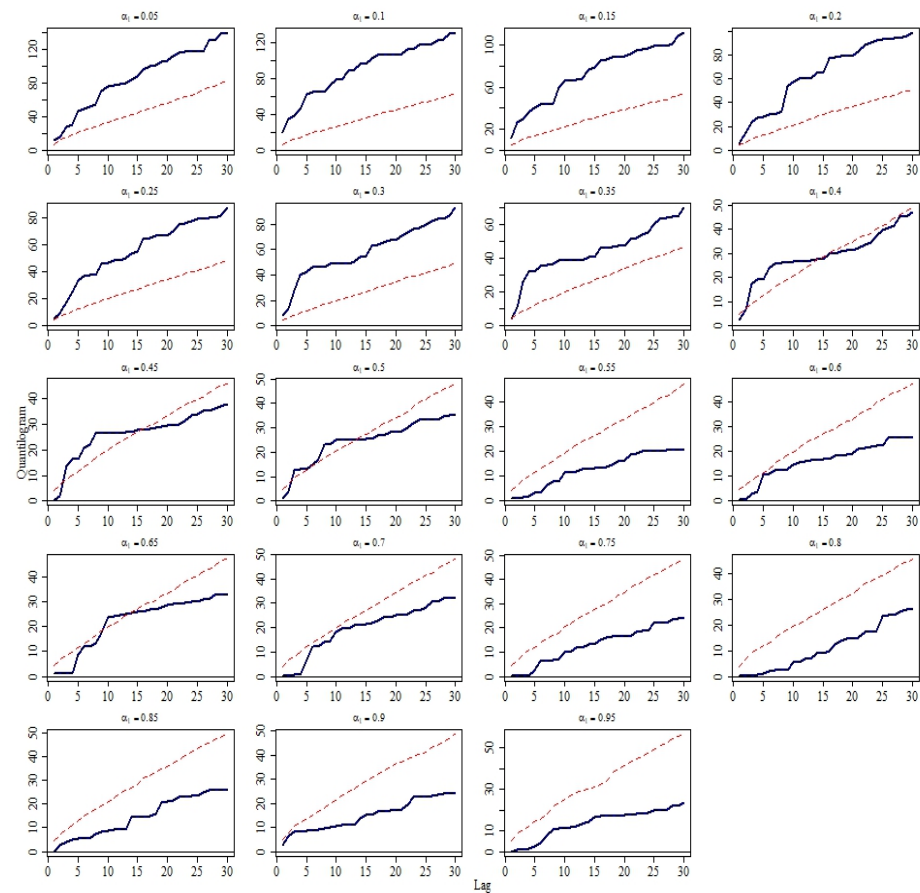


Figure 4. Box-Ljung test statistic $\hat{Q}_\alpha^{(p)}$ for each lag p using $\hat{\rho}_\alpha(k)$, to capture directional predictability from WTI to OVX, when both return series are in the same quantiles. The dashed lines are the 95% bootstrap confidence intervals.

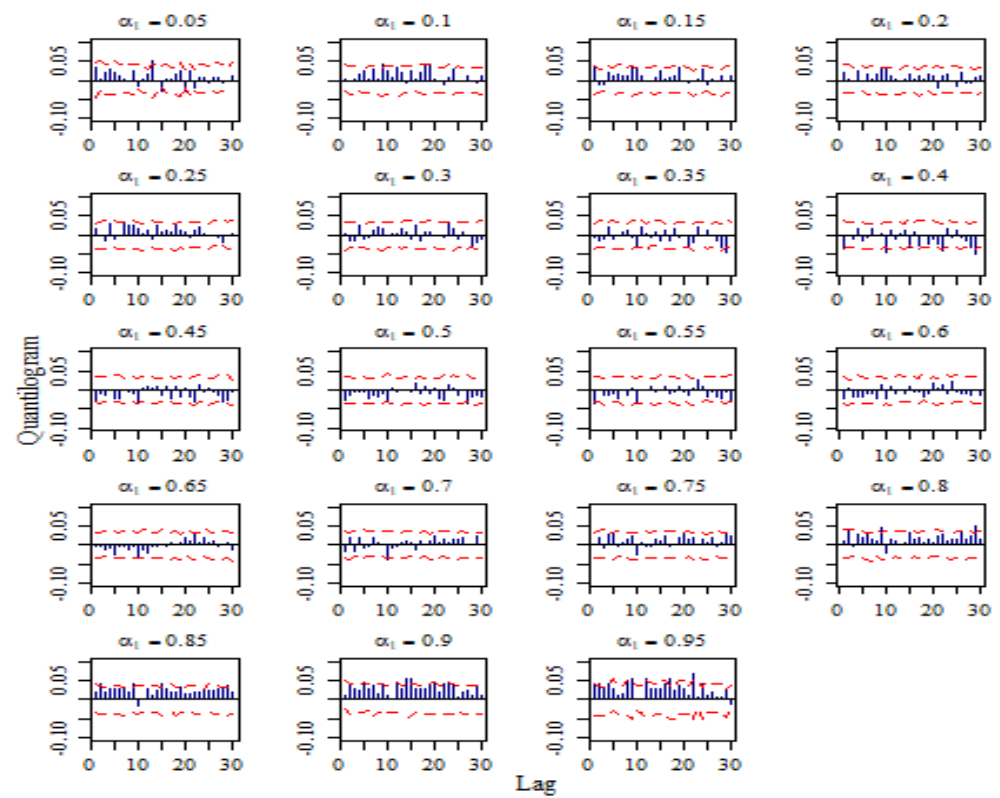


Figure 5. Sample cross-quantilograms, to capture directional predictability from OVX to oil, when both return series are in the same quantiles. See notes to Figure 3.

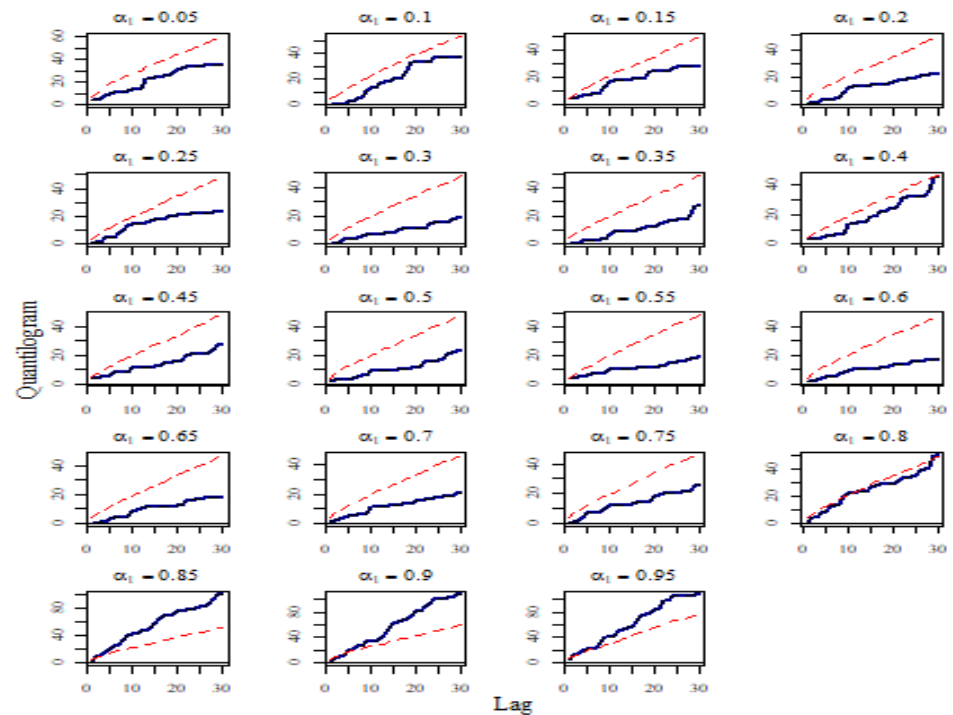


Figure 6. Box-Ljung test statistic $\hat{Q}_\alpha^{(p)}$ for each lag p using $\hat{\rho}_\alpha(k)$, to capture directional predictability from OVX to WTI, when both return series are in the same quantiles. See notes to Figure 4.

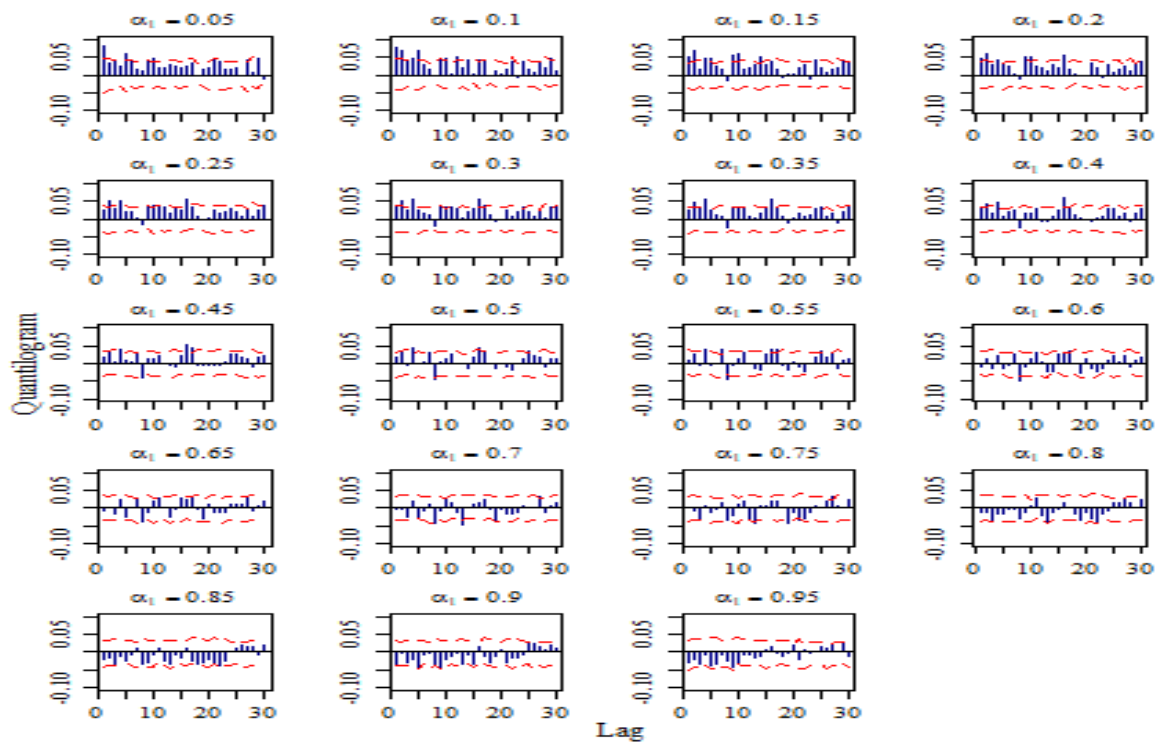


Figure 7. Sample cross-quantilograms for WTI returns in the lower quantile, i.e., $q_2(\alpha_2)$ for $\alpha_2 = 0.1$, to capture directional predictability from WTI return to OVX. See notes to Figure 3.

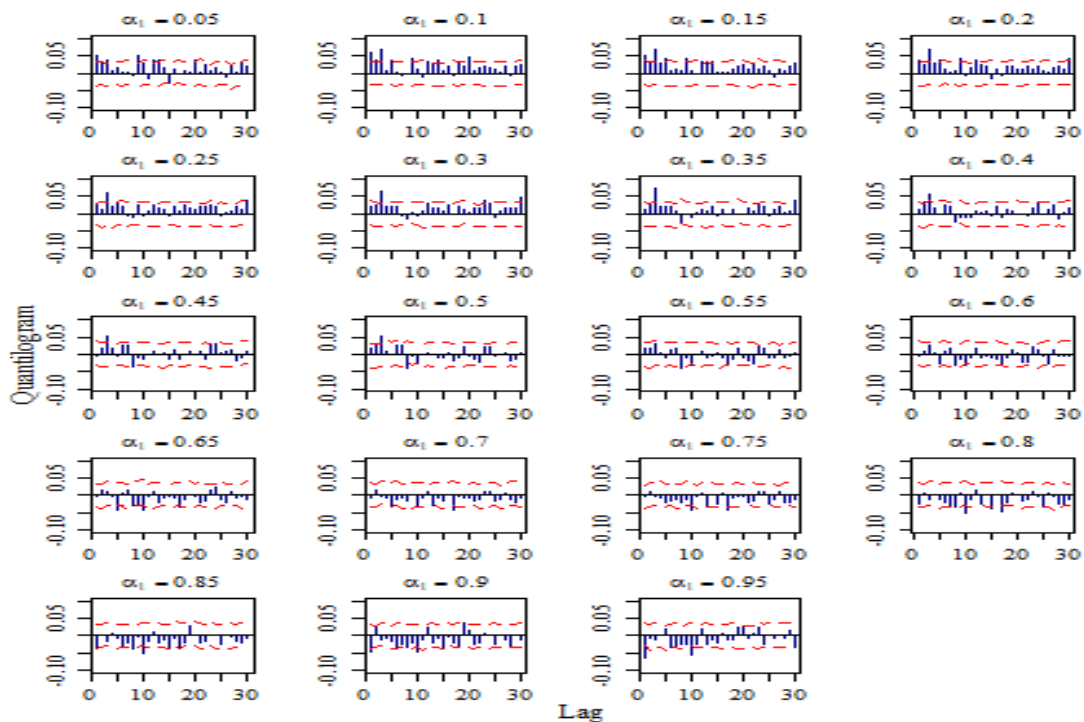


Figure 8. Sample cross-quantilograms for WTI returns in the median quantile, i.e., $q_2(\alpha_2)$ for $\alpha_2 = 0.5$, to capture directional predictability from WTI to OVX returns. See notes to Figure 3.

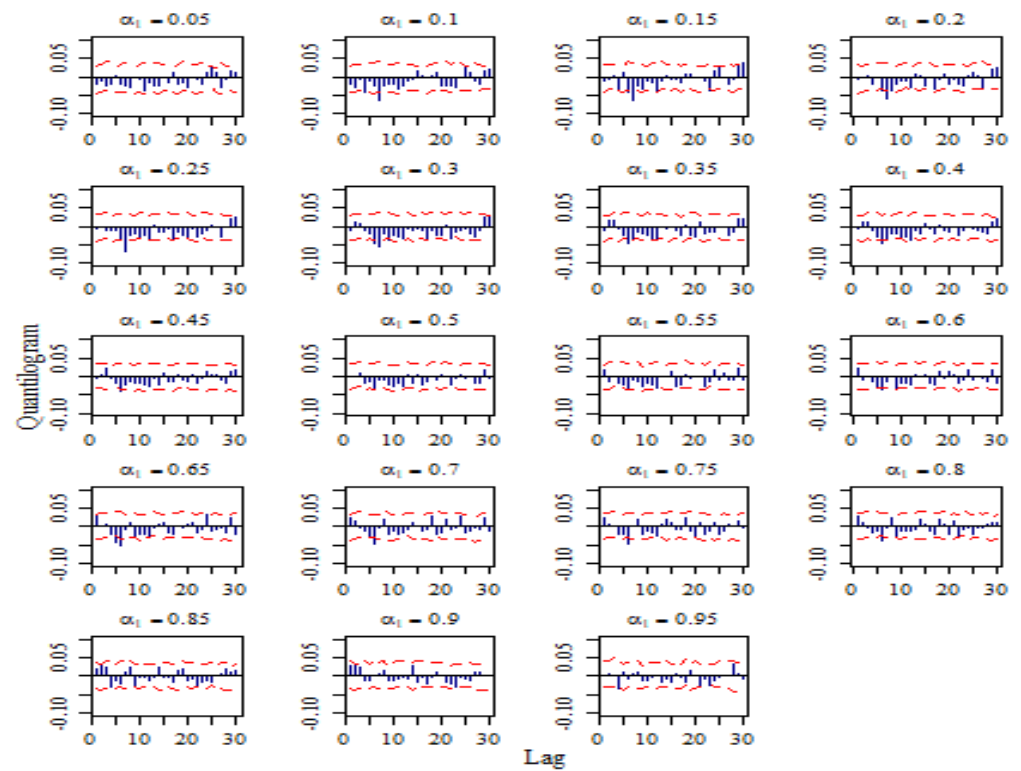


Figure 9. Sample cross-quantilograms for WTI returns in the upper quantile, i.e., $q_2(\alpha_2)$ for $\alpha_2 = 0.9$ and OVX in the other 19 quantiles, i.e., $q_1(\alpha_1)$ for $\alpha_1 \in \{0.05, 0.10, \dots, 0.95\}$. See notes to Figure 3.

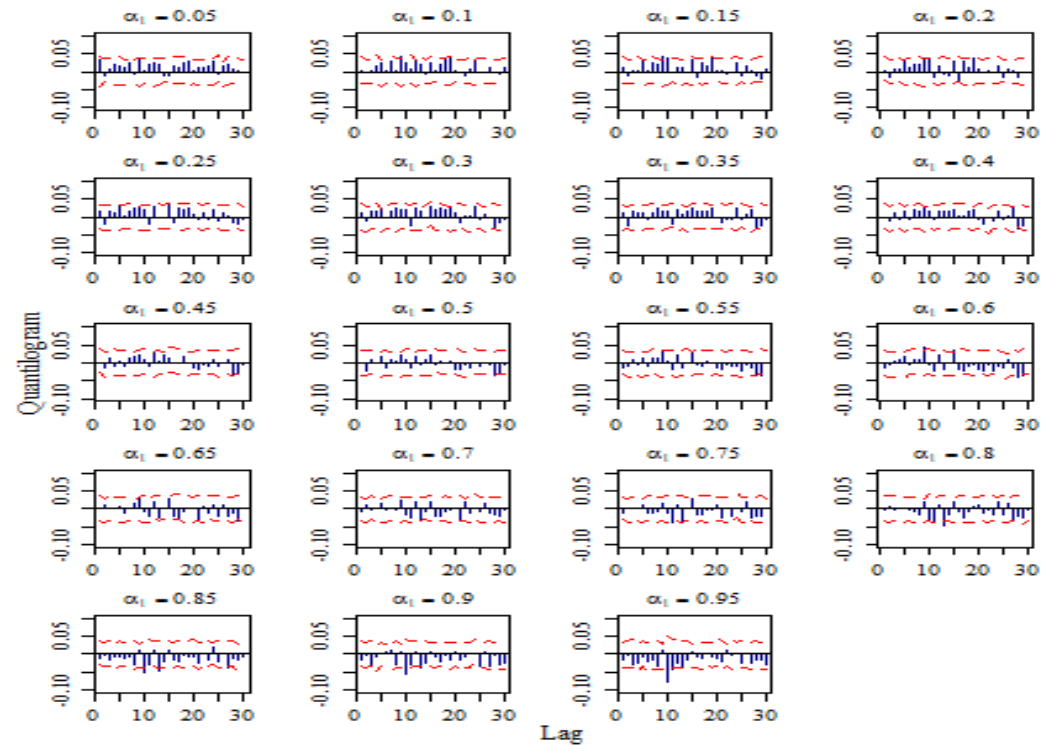


Figure 10. Sample cross-quantilograms for OVX returns in the lower quantile, i.e., $q_2(\alpha_2)$ for $\alpha_2 = 0.1$, to capture directional predictability from OVX to WTI returns. See notes to Figure 3.

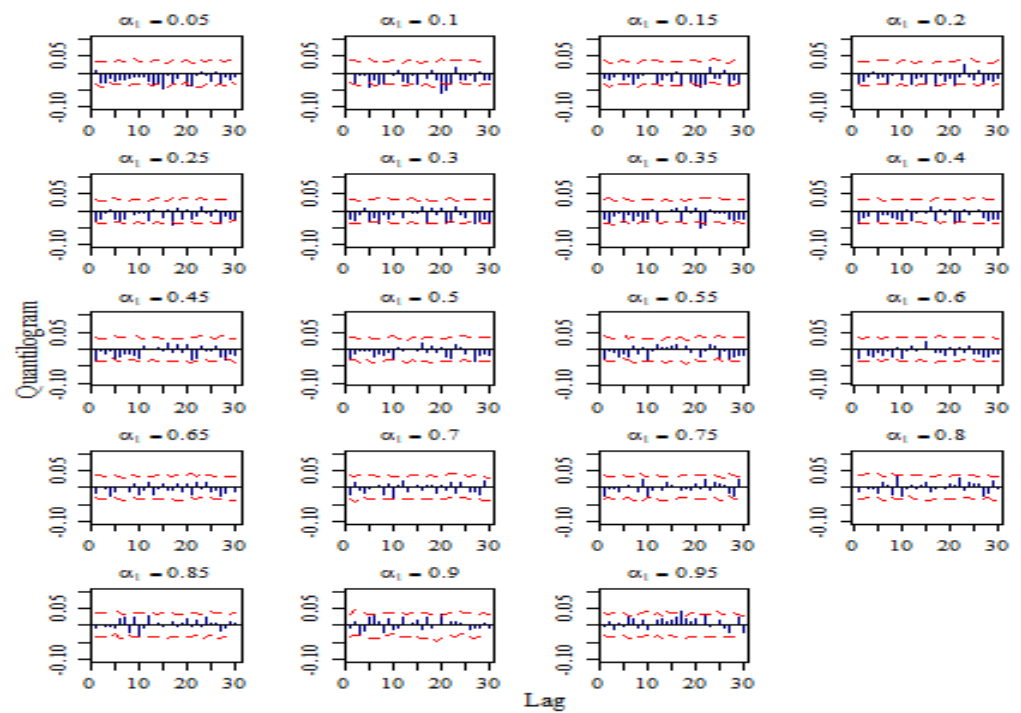


Figure 11. Sample cross-quantilograms for OVX returns in the median quantile, i.e., $q_2(\alpha_2)$ for $\alpha_2 = 0.5$, to capture directional predictability from OVX to WTI returns. See notes to Figure 3.

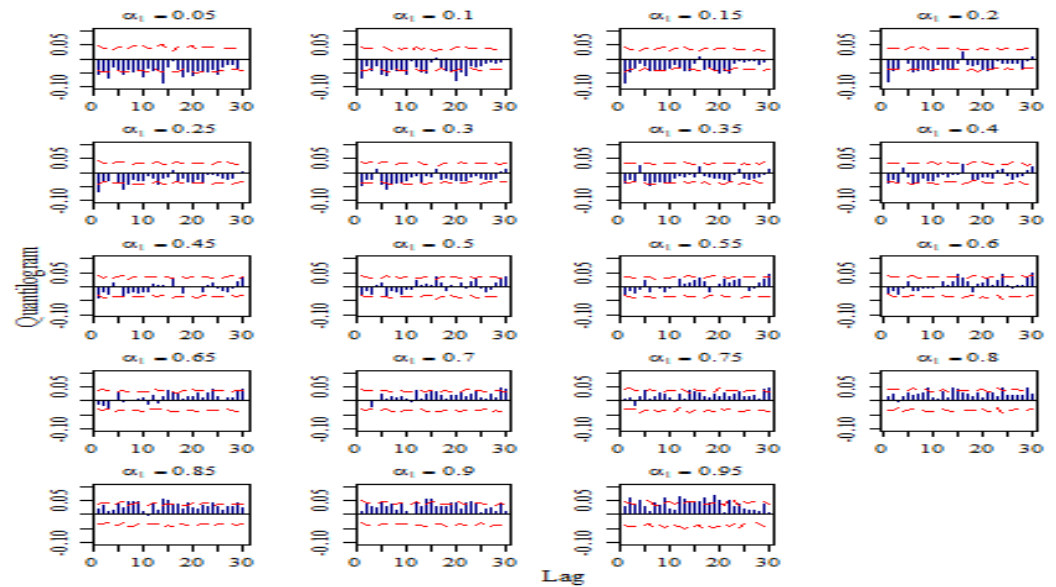


Figure 12. Sample cross-quantilograms for OVX returns in the upper quantile, i.e., $q_2(\alpha_2)$ for $\alpha_2 = 0.9$, to capture directional predictability from OVX to WTI returns. See notes to Figure 3.

Based on the above analysis, we reveal the quantile dependence between the two return series when both are in the same quantiles, and generally find that OVX (WTI) tends to co-crash (boom) with WTI (OVX). Furthermore, the dependence between both return series is essentially found to be significant when both return series are in the tails of the distribution.

We next examine the interdependence between OVX and WTI returns when the returns series are in opposite quantiles.

5.2.2. Results When the Return Series Are in Opposite Quantiles

To capture the potential quantile dependence and directional predictability of one series to the other when the return series are in opposite quantiles, we present the cross-quantilogram of lag

$k = 1, 2, \dots, 30$ when the distributions of the series returns are in bear, bull, and normal states, i.e., three quantiles are considered: low ($\tau = 0.1$), high ($\tau = 0.9$), and median ($\tau = 0.5$). The full results for other quantiles and the Box–Ljung test statistic results are available from the authors upon request.

We first provide the results (Figure 7) of the cross-quantilogram when the WTI returns are in the lower quantile, i.e., $q_2(\alpha_2)$ for $\alpha_2 = 0.1$, and the OVX returns are in the other 19 quantiles, i.e., $q_1(\alpha_1)$ for $\alpha_1 \in \{0.05, 0.10, \dots, 0.95\}$. OVX is found to have a dependence of negative and positive signs on WTI. This outcome, though, is mainly significant in the lower quantiles, suggesting that the structure of dependence between the two series is mostly seen during the low OVX state. Next, we consider the scenario when WTI returns are in the median quantile, i.e., $q_2(\alpha_2)$ for $\alpha_2 = 0.5$, with positive (negative) and significant cross-quantilogram estimates, for some lags, at the upper (lower) quantiles of OVX returns (see Figure 8). When WTI returns are lower than the median, OVX returns have a positive (negative) dependence on WTI returns in the lower (upper) quantiles. Finally, we present the upper quantile scenario, when oil returns are in the higher quantile, $q_2(\alpha_2) = 0.9$, and OVX returns are in the other 19 quantiles, i.e., $q_1(\alpha_1)$ for $\alpha_1 \in \{0.05, 0.10, \dots, 0.95\}$. In Figure 9, we see evidence of spillovers from WTI returns to OVX returns. Overall, there is no consistency in either the sign or the pattern of the cross-quantilogram estimates. Furthermore, a significant negative dependence is only seen for some lower quantiles of OVX returns. This suggests that the relationship between the two return series is very weak. Interestingly, a comparison of Figures 7–9 reveals that the predictive ability of WTI returns over OVX returns is usually more noticeable during bearish market conditions.

In the case where OVX returns are in the lower quantile, i.e., $q_2(\alpha_2)$ for $\alpha_2 = 0.1$ and WTI returns are the other 19 quantiles, i.e., $q_1(\alpha_1)$ for $\alpha_1 \in \{0.05, 0.10, \dots, 0.95\}$, the results are given in Figure 10. Overall, the sample cross-quantilograms are statistically insignificant, suggesting that no significant dependence exists between WTI returns and OVX returns when the latter is in lower quantiles. Similarly, once the OVX returns are at the medium quantile (Figure 11), there is no sufficient indication justifying the quantile association between the return series. This advocates that, once OVX is in a normal condition, OVX returns do not have the ability to predict WTI returns.

Figure 12 shows that when OVX is in the higher quantile, $q_2(\alpha_2) = 0.9$, the cross-quantilogram estimates are negative (positive) and statistically significant for some lags in the lower (upper) quantiles. This outcome indicates that when OVX returns are very high, revealing rising uncertainty in the crude oil market, OVX returns exhibit a substantial impact on WTI returns. However, this impact is only found in the extreme quantiles (very bearish or very bullish conditions) of oil price returns. A comparison of Figures 10–12 shows that the forecasting ability of OVX returns over WTI returns is usually more pronounced during soaring investor sentiment about the state of the crude oil market.

To sum up, the results indicate that when WTI and OVX return series are in different quantiles, WTI returns can be useful to predict extreme low/high variations in OVX returns during bearish market conditions. Indeed, they show that the lower quantile of WTI returns positively and significantly influences the quantiles of OVX returns, but the dependence is reversed during bear market conditions. Under normal market circumstances, the dependence can be either positive or negative. These results are quite comparable to Benedetto et al. [33], who present evidence of predictability from OVX to WTI, although our results are more nuanced and account for upper, middle, and lower quantiles. For the reverse relationship, OVX returns are found to be helpful in predicting extreme fluctuations in WTI returns. Indeed, evidence indicates that high OVX returns have significant and negative effects on the lower quantiles of WTI returns, but the dependence turns positive at upper quantiles. Furthermore, during low and middle OVX returns, the evidence does not support any directional predictability, which validates the results of Liu et al. [21], who show that oil price returns are reacting more to OVX increase than to OVX decrease. This also confirms the findings of Agbeyegbe [41] and Ji and Fan [27], who postulate that OVX is favored as a gauge of investor fear over risk preference.

Broadly, our findings prove that the relationships between OVX and oil prices exhibit heterogeneous behavior across quantiles and asymmetric dependence. These findings are partly in line with Agbeyegbe [41], Chen and Zou [57], Silva Junior [45], Lin and Tsai [40], Shaikh [44], and Fousekis [46], who show evidence of asymmetric relationships between OVX and oil prices. Furthermore, our findings are partly in accordance with Aboura and Chevallier [38], who establish the existence of an inverse leverage effect, which characterizes a larger increase in volatility following an upsurge in oil prices than following a decrease in oil prices of the same magnitude. However, the findings do not agree with Chen et al. [39], who find that a feeble negative association exists between OVX changes and future crude oil price returns, and that extreme levels of OVX cannot appropriately forecast future fluctuations of returns. However, it is worth noting that the studies mentioned above do not

rely on quantile approaches as we do, particularly in relation to causal links between the two return series. Our comprehensive analysis allows us to cover the detailed interplay between oil prices and oil implied volatility.

6. Conclusions

In this study, we analyze the Granger causal interplay and directional predictability between crude oil returns and the returns of the Crude Oil Volatility Index (OVX), under various market conditions. To this end, we apply various quantile-based tests and models, specifically the quantile unit root test developed by Galvao [47], the parametric test of Granger causality in quantiles of Troster [48], and the nonparametric cross-quantilogram approach of Han et al. [49].

While the Granger causality in quantiles analysis indicates a significant bi-directional predictability between oil returns and OVX returns, the results of the cross-quantilogram approach show a complete and more nuanced picture of the relationships at various quantiles. Specifically, the relationship exhibits heterogeneous behavior, which points to asymmetry across quantiles. Furthermore, the quantile dependence from oil returns to OVX returns is different from that from OVX returns to WTI returns. The predictive power of oil returns is generally seen when both return series are in similar lower quantiles, which means that when the oil market is bearish, it is possible for OVX to be declining. In opposite quantiles, however, there is evidence of quantile predictability at the middle quantile and at the tails of oil returns, particularly the left tail.

For the reverse relationship, OVX returns can be used to predict extreme low/high variations in WTI prices. Precisely, when the level of OVX is high, OVX returns have a negative and significant effect on the lower quantiles of oil returns. However, this dependence turns positive at the upper quantiles of oil returns. At middle and low OVX return quantiles, there is no evidence of directional predictability. The existence of causal links in tails advocates the adequacy and significance of our modelling strategy, which casts doubt on the suitability of the conventional conditional mean-founded causality models that give a partial picture of the WTI-OVX relationship.

The findings of the study are useful for investors in the oil market, as they offer a new perspective on the relationship between return and volatility in the market and point to the asymmetric dependence across quantiles. Although several previous studies present evidence of a significant relationship between oil returns and OVX, the innovation of our study is that it reveals that the causality is quantile-dependent and asymmetric. As a result, investors aiming to control the evolution of prices should take the level of implied volatility into account, because the level of investor sentiment in the oil market, measured by OVX, may drive upcoming variations in spot crude oil returns at some quantiles. At the same time, spot oil price fluctuations can affect implied volatility levels under specific conditions.

The results are also relevant to portfolio risk management and the hedging strategies of participants in the crude oil market. For example, investors can better forecast the return and volatility of the oil market, conditional on market states, and thus refine their trading and hedging strategies and assess their exposure to oil market risk. Additionally, they can anticipate variations in their oil portfolio values due to oil volatility shocks, and can thus adjust their investment and trading positions, considering crude oil market states such as extremely unstable or stable markets. More precisely, investors should consider an asymmetric hedging strategy under upside and downside variations in the levels of OVX, particularly extreme movements of OVX upset by oil-related events that increase the uncertainty and complexity of the international oil market.

Given that the quantile dependence between crude oil prices and oil implied volatility may depend on multitude exogenous variables, future studies could extend this research by accounting for the effect of other variables such as US stock market conditions.

Author Contributions: B.R. conceptualized the paper, investigated and provided all resources, defined the research methodology, performed the estimation and analysis, and wrote the original draft preparation. E.B. supervised the project, contributed to the interpretation of the results, and revised the final manuscript. All authors have read and agreed to the published version of the manuscript.

Funding: The authors declare that no funds, grants, or other support were received during the preparation of this manuscript.

Data Availability Statement: The datasets used and analyzed during the study are available from public websites.

Conflicts of Interest: The authors declare no competing interest.

References

1. Aguilera, R.F.; Eggert, R.G.; CC, G.L.; Tilton, J.E. Depletion and the future availability of petroleum resources. *Energy J.* **2009**, *30*, 141–174. [[CrossRef](#)]
2. Demirbas, A.; Omar Al-Sasi, B.; Nizami, A.S. Recent volatility in the price of crude oil. *Energy Sources Part B Econ. Plan. Policy* **2017**, *12*, 408–414. [[CrossRef](#)]
3. Joo, Y.C.; Park, S.Y. Oil prices and stock markets: Does the effect of uncertainty change over time? *Energy Econ.* **2017**, *61*, 42–51. [[CrossRef](#)]
4. Bouri, E.; Demirel, R.; Gupta, R.; Pierdzioch, C. Infectious diseases, market uncertainty and oil market volatility. *Energies* **2020**, *13*, 4090. [[CrossRef](#)]
5. Dutta, A.; Bouri, E.; Noor, M.H. Climate bond, stock, gold, and oil markets: Dynamic correlations and hedging analyses during the COVID-19 outbreak. *Resour. Policy* **2021**, *74*, 102265. [[CrossRef](#)] [[PubMed](#)]
6. Diaz, E.M.; Molero, J.C.; Perez de Gracia, F. Oil price volatility and stock returns in the G7 economies. *Energy Econ.* **2016**, *54*, 417–430. [[CrossRef](#)]
7. Luo, X.; Qin, S. Oil price uncertainty and Chinese stock returns: New evidence from the oil volatility index. *Finance Res. Lett.* **2017**, *20*, 29–34. [[CrossRef](#)]
8. Kinatader, H.; Wagner, N. Oil and Stock Market Returns: Direction, Volatility, or Liquidity? *SSRN Electron. J.* **2017**. [[CrossRef](#)]
9. Batten, J.A.; Kinatader, H.; Szilagyi, P.G.; Wagner, N.F. Liquidity, surprise volume and return premia in the oil market. *Energy Econ.* **2019**, *77*, 93–104. [[CrossRef](#)]
10. Szakmary, A.; Ors, E.; Kyoung Kim, J.; Davidson, W.N. The predictive power of implied volatility: Evidence from 35 futures markets. *J. Bank. Finance* **2003**, *27*, 2151–2175. [[CrossRef](#)]
11. Becker, R.; Clements, A.E.; White, S.I. Does implied volatility provide any information beyond that captured in model-based volatility forecasts? *J. Bank. Finance* **2007**, *31*, 2535–2549. [[CrossRef](#)]
12. Mencía, J.; Sentana, E. Valuation of VIX derivatives. *J. Finance Econ.* **2013**, *108*, 367–391. [[CrossRef](#)]
13. Liu, Z.; Tseng, H.K.; Wu, J.S.; Ding, Z. Implied volatility relationships between crude oil and the U.S. stock markets: Dynamic correlation and spillover effects. *Resour. Policy* **2020**, *66*, 101637. [[CrossRef](#)]
14. Dutta, A.; Bouri, E.; Saeed, T. News-based equity market uncertainty and crude oil volatility. *Energy* **2021**, *222*, 119930. [[CrossRef](#)]
15. Lanne, M.; Saikkonen, P. Modeling the U.S. Short-Term Interest Rate by Mixture Autoregressive Processes. *SSRN Electron. J.* **2005**, *1*, 96–125. [[CrossRef](#)]
16. Ali, F.D.; Bin, L.; Leqin, W. Revisiting the risk-return relation in the South African stock market. *Afr. J. Bus. Manag.* **2012**, *6*, 11411–11415. [[CrossRef](#)]
17. Chang, K.L. Does the return-state-varying relationship between risk and return matter in modeling the time series process of stock return? *Int. Rev. Econ. Finance* **2016**, *42*, 72–87. [[CrossRef](#)]
18. Aslanidis, N.; Christiansen, C.; Savva, C.S. Risk-return trade-off for European stock markets. *Int. Rev. Finance Anal.* **2016**, *46*, 84–103. [[CrossRef](#)]
19. Abakah, E.J.A.; Tiwari, A.K.; Alagidede, I.P.; Gil-Alana, L.A. Re-examination of risk-return dynamics in international equity markets and the role of policy uncertainty, geopolitical risk and VIX: Evidence using Markov-switching copulas. *Finance Res. Lett.* **2022**, *47*, 102535. [[CrossRef](#)]
20. Lundblad, C. The risk return tradeoff in the long run: 1836–2003. *J. Finance Econ.* **2007**, *85*, 123–150. [[CrossRef](#)]
21. Liu, B.; Ji, Q.; Fan, Y. Dynamic return-volatility dependence and risk measure of CoVaR in the oil market: A time-varying mixed copula model. *Energy Econ.* **2017**, *68*, 53–65. [[CrossRef](#)]
22. Wu, S.-J.; Lee, W.-M. Intertemporal risk–return relationships in bull and bear markets. *Int. Rev. Econ. Finance* **2015**, *38*, 308–325. [[CrossRef](#)]
23. Glosten, L.R.; Jagannathan, R.; Runkle, D.E.; Breen, W.; Hansen, L.; Hess, P.; Hsieh, D.; Judson, R.; Kocher-Lakota, N.; McDonald, R.; et al. On the Relation between the Expected Value and the Volatility of the Nominal Excess Return on Stocks. *J. Finance* **1993**, *48*, 1779–1801. [[CrossRef](#)]
24. Bollerslev, T.; Osterrieder, D.; Sizova, N.; Tauchen, G. Risk and return: Long-run relations, fractional cointegration, and return predictability. *J. Finance Econ.* **2013**, *108*, 409–424. [[CrossRef](#)]
25. Chen, M. Risk-return tradeoff in Chinese stock markets: Some recent evidence. *Int. J. Emerg. Mark.* **2015**, *10*, 448–473. [[CrossRef](#)]
26. Basher, S.A.; Sadorsky, P. Hedging emerging market stock prices with oil, gold, VIX, and bonds: A comparison between DCC, ADCC and GO-GARCH. *Energy Econ.* **2016**, *54*, 235–247. [[CrossRef](#)]
27. Ji, Q.; Fan, Y. Modelling the joint dynamics of oil prices and investor fear gauge. *Res. Int. Bus. Finance* **2016**, *37*, 242–251. [[CrossRef](#)]
28. Haugom, E.; Langeland, H.; Molnár, P.; Westgaard, S. Forecasting volatility of the U.S. oil market. *J. Bank. Finance* **2014**, *47*, 1–14. [[CrossRef](#)]
29. Lux, T.; Segnon, M.; Gupta, R. Forecasting crude oil price volatility and value-at-risk: Evidence from historical and recent data. *Energy Econ.* **2016**, *56*, 117–133. [[CrossRef](#)]
30. Dutta, A. Modeling and forecasting oil price risk: The role of implied volatility index. *J. Econ. Stud.* **2017**, *44*, 1003–1016. [[CrossRef](#)]
31. Lv, W. Does the OVX matter for volatility forecasting? Evidence from the crude oil market. *Phys. A Stat. Mech. Its Appl.* **2018**, *492*, 916–922. [[CrossRef](#)]

32. Chen, H.; Liu, L.; Li, X. The predictive content of CBOE crude oil volatility index. *Phys. A Stat. Mech. Its Appl.* **2018**, *492*, 837–850. [[CrossRef](#)]
33. Benedetto, F.; Mastroeni, L.; Quaresima, G.; Vellucci, P. Does OVX affect WTI and Brent oil spot variance? Evidence from an entropy analysis. *Energy Econ.* **2020**, *89*, 104815. [[CrossRef](#)]
34. Maghyereh, A.I.; Awartani, B.; Bouri, E. The directional volatility connectedness between crude oil and equity markets: New evidence from implied volatility indexes. *Energy Econ.* **2016**, *57*, 78–93. [[CrossRef](#)]
35. Bouri, E.; Jain, A.; Biswal, P.C.; Roubaud, D. Cointegration and nonlinear causality amongst gold, oil, and the Indian stock market: Evidence from implied volatility indices. *Resour. Policy* **2017**, *52*, 201–206. [[CrossRef](#)]
36. Choi, S.Y.; Hong, C. Relationship between uncertainty in the oil and stock markets before and after the shale gas revolution: Evidence from the OVX, VIX, and VKOSPI volatility indices. *PLoS ONE* **2020**, *15*, e0232508. [[CrossRef](#)] [[PubMed](#)]
37. Naeem, M.A.; Hasan, M.; Agyemang, A.; Chowdhury, M.I.H.; Balli, F. Time-frequency dynamics between fear connectedness of stocks and alternative assets. *Int. J. Finance Econ.* **2021**, 1–14. [[CrossRef](#)]
38. Aboura, S.; Chevallier, J. Leverage vs. feedback: Which effect drives the oil market? *Finance Res. Lett.* **2013**, *10*, 131–141. [[CrossRef](#)]
39. Chen, Y.; He, K.; Yu, L. The Information Content of OVX for Crude Oil Returns Analysis and Risk Measurement: Evidence from the Kalman Filter Model. *Ann. Data Sci.* **2015**, *2*, 471–487. [[CrossRef](#)]
40. Lin, J.B.; Tsai, W. The relations of oil price change with fear gauges in global political and economic environment. *Energies* **2019**, *12*, 2982. [[CrossRef](#)]
41. Agbeyegbe, T.D. An inverted U-shaped crude oil price return-implied volatility relationship. *Rev. Finance Econ.* **2015**, *27*, 28–45. [[CrossRef](#)]
42. Echaust, K.; Just, M. Tail dependence between crude oil volatility index and WTI oil price movements during the COVID-19 pandemic. *Energies* **2021**, *14*, 4147. [[CrossRef](#)]
43. Li, S.; Li, J.; Lu, X.; Sun, Y. Exploring the dynamic nonlinear relationship between crude oil price and implied volatility indices: A new perspective from MMV-MFDFA. *Phys. A Stat. Mech. Its Appl.* **2022**, *603*, 127684. [[CrossRef](#)]
44. Shaikh, I. The relation between implied volatility index and crude oil prices. *Eng. Econ.* **2019**, *30*, 556–566. [[CrossRef](#)]
45. Silva, J.C.A., Jr. An S-Shaped Crude Oil Price Return-Implied Volatility Relation: Parametric and Nonparametric Estimations. *Int. J. Econ. Finance* **2017**, *9*, 54. [[CrossRef](#)]
46. Fousekis, P. Crude oil price and implied volatility: Insights from non-parametric quantile regressions. *Stud. Econ. Finance* **2019**, *36*, 168–182. [[CrossRef](#)]
47. Galvao, A.F. Unit root quantile autoregression testing using covariates. *J. Econom.* **2009**, *152*, 165–178. [[CrossRef](#)]
48. Troster, V. Testing for Granger-causality in quantiles. *Econom. Rev.* **2018**, *37*, 850–866. [[CrossRef](#)]
49. Han, H.; Linton, O.; Oka, T.; Whang, Y. The Cross-Quantilegram: Measuring Quantile Dependence and Testing Directional Predictability between Time Series. *J. Econom.* **2016**, *193*, 251–270. [[CrossRef](#)]
50. Yang, M. Journal of Economic Dynamics & Control The risk return relationship: Evidence from index returns and realised variances. *J. Econ. Dyn. Control* **2019**, *107*, 103732. [[CrossRef](#)]
51. Agnolucci, P. Volatility in crude oil futures: A comparison of the predictive ability of GARCH and implied volatility models. *Energy Econ.* **2009**, *31*, 316–321. [[CrossRef](#)]
52. Herrera, A.M.; Karaki, M.B. The effects of oil price shocks on job reallocation. *J. Econ. Dyn. Control.* **2015**, *61*, 95–113. [[CrossRef](#)]
53. Herrera, A.M.; Karaki, M.B.; Rangaraju, S.K. Where do jobs go when oil prices drop? *Energy Econ.* **2017**, *64*, 469–482. [[CrossRef](#)]
54. Karaki, M.B. Nonlinearities in the response of real GDP to oil price shocks. *Econ. Lett.* **2017**, *161*, 146–148. [[CrossRef](#)]
55. Bahel, E.; Marrouch, W.; Gaudet, G. The economics of oil, biofuel and food commodities. *Resour. Energy Econ.* **2013**, *35*, 599–617. [[CrossRef](#)]
56. Ma, F.; Wahab, M.I.M.; Huang, D.; Xu, W. Forecasting the realized volatility of the oil futures market: A regime switching approach. *Energy Econ.* **2017**, *67*, 136–145. [[CrossRef](#)]
57. Chen, Y.; Zou, Y. Examination on the Relationship between OVX and Crude Oil Price with Kalman Filter. *Procedia Comput. Sci.* **2015**, *55*, 1359–1365. [[CrossRef](#)]
58. Raggad, B. Can implied volatility predict returns on oil market? Evidence from Cross-Quantilegram Approach. *Resour. Policy* **2023**, *80*, 103277. [[CrossRef](#)]
59. Koenker, R.; Xiao, Z. Unit root quantile autoregression inference. *J. Am. Stat. Assoc.* **2004**, *99*, 775–787. [[CrossRef](#)]
60. Troster, V.; Shahbaz, M.; Uddin, G.S. Renewable energy, oil prices, and economic activity: A Granger-causality in quantiles analysis. *Energy Econ.* **2018**, *70*, 440–452. [[CrossRef](#)]
61. Ye, C.; Chen, Y.; Inglesi-Lotz, R.; Chang, T. CO₂ emissions converge in China and G7 countries? Further evidence from Fourier quantile unit root test. *Energy Environ.* **2020**, *31*, 348–363. [[CrossRef](#)]
62. Sakov, A.; Bickel, P.J. An Edgeworth expansion for the m out of n bootstrapped median. *Stat. Probab. Lett.* **2000**, *49*, 217–223. [[CrossRef](#)]
63. Broock, W.A.; Scheinkman, J.A.; Dechert, W.D.; LeBaron, B. A test for independence based on the correlation dimension. *Econom. Rev.* **1996**, *15*, 197–235. [[CrossRef](#)]
64. Bai, J.; Perron, P. Computation and analysis of multiple structural change models. *J. Appl. Econom.* **2003**, *18*, 1–22. [[CrossRef](#)]
65. Dickey, D.A.; Fuller, W.A. Distribution of the Estimators for Autoregressive Time Series with a Unit Root. *J. Am. Stat. Assoc.* **1979**, *74*, 427–431. [[CrossRef](#)]

66. Phillips, P.C.B.; Perron, P. Testing for a unit root in time series regression. *Biometrika* **1988**, *75*, 335–346. [[CrossRef](#)]
67. Zivot, E.; Andrews, D.W.K. Further evidence on the Great Crash, the oil-price shock, and the and Unit-Root hypothesis. *J. Bus. Econ. Stat.* **1992**, *10*, 251–270.
68. Johansen, S. Estimation and Hypothesis Testing of Cointegration Vectors in Gaussian Vector Autoregressive Models. *Econometrica* **1991**, *59*, 1551–1580. [[CrossRef](#)]
69. Johansen, S. *Likelihood-Based Inference in Cointegrated Vector Autoregressive Models*; Oxford University Press: Oxford, UK, 1995.
70. Xiao, Z. Quantile cointegrating regression. *J. Econom.* **2009**, *150*, 248–260. [[CrossRef](#)]
71. Lin, J.B.; Liang, C.C.; Tsai, W. Nonlinear relationships between oil prices and implied volatilities: Providing more valuable information. *Sustainability* **2019**, *11*, 3906. [[CrossRef](#)]

Disclaimer/Publisher’s Note: The statements, opinions and data contained in all publications are solely those of the individual author(s) and contributor(s) and not of MDPI and/or the editor(s). MDPI and/or the editor(s) disclaim responsibility for any injury to people or property resulting from any ideas, methods, instructions or products referred to in the content.